Understanding Damage Propagation in UHMWPE Composite Armour Plate on Successive Impacts by 7.62 mm Projectiles

Kartikeya Kartikeya[1], Mohit Garg[1], Rajesh Punia[1] Khushi Ram[1,] and **Naresh Bhatnagar**[1]

[1]*Department of Mechanical Engineering, Indian Institute of Technology Delhi, Hauz Khas, New Delhi – 110016, India*
nareshb@mech.iitd.ac.in

Abstract. The UHMWPE composite armour plates are extensively used to defeat 7.62 mm mild steel and lead core projectiles. However, after the first impact, the armour is weakened for subsequent impacts due to plate delamination associated with each impact. In this work, two identical UHMWPE composite armour plates were subjected to eight high-velocity impacts of 7.62 × 39 mm mild steel core (MSC) and 7.62 × 51 mm lead core (LC) projectiles. The delamination damage is quantified using ultrasonic C-Scans and Back Face Signature (BFS). It was noticed that both MSC and LC projectiles (8 shots) were defeated by UHMWPE composite armour. However, the damage inflicted by LC projectiles on an armour plate was considerably higher than by MSC projectiles. The cores of LC projectiles were destroyed during impact but the cores of MSC projectiles were retrieved and studied for steel deformation.

1. INTRODUCTION

Modern personal body armour is a lifesaver for security personnel. Personal body armour is typically made of multiple materials, given the diverse nature of threats. Hard armour plates (HAP) defeat high-velocity ammunition. These HAPs are typically fabricated from ultra-high molecular weight (UHMWPE) fibre-reinforced polymer composites and are added with either a hardened steel or ceramic strike face to defeat hardened core projectiles [1]. The UHMWPE composite armours are lightweight and provide excellent ballistic penetration resistance [2–4]. The HAPs from UHMWPE composite are generally fabricated by compression moulding [5–7].

Lee et al. [8] conducted one of the first impact studies on UHMWPE composite, Spectra® fibre-reinforced laminates. The authors noted that unidirectional fibre-reinforced composites performed better than woven fabric-reinforced composites. Taylor and Carr [9] observed that non-perforated UHMWPE composite panels showed extensive delamination whereas perforated specimens exhibited plugging and deformation. Karthikeyan et al. [10] conducted a study to understand the deformation and failure of UHMWPE fibre-reinforced laminates in comparison with carbon fibre-reinforced composite plastic (CFRP) laminates using the Moiré shadow technique. The UHMWPE laminates showed progressive delamination and failure and the CFRP laminates exhibited elastic behaviour till failure. The authors noted that UHMWPE laminate with the lowest shear strength matrix had the highest ballistic limit.

Heisserer et al.[11] observed that the depth of penetration in the UHMWPE composites had a linear relationship with the kinetic energy of the projectiles. They also observed that the amount of energy absorbed from perforated projectiles was similar in all cases showing that UHMWPE composite can absorb only a certain amount of energy. Nguyen et al. [12] compared V_{50} of thick UHMWPE composites with armour steel, aluminium and other fibre-reinforced composites using 12.7 mm and 20 mm FSPs. It was noticed that the UHMWPE composites were less space efficient than steels and glass fibre-reinforced composites, however, the UHMWPE composites were much more efficient than other tested materials. For thicker targets, the authors showed that the failure is a two-step process i.e., shear failure on the front surface up to a certain depth and membrane stretching on the back surface. Lassig et al. [13] showed that laminates fabricated at higher pressure had significantly improved ballistic limits. The plate planar impact tests were also carried out to determine the shock equation of state (EOS). The effect of consolidation pressure on shock EOS was evident below particle velocity of 1100 m s^{-1}.

Reddy et al. [14] subjected various 20 mm thick UHMWPE composites to impact by 7.62 × 39 mm MSC projectiles. The laminates had different hybridization using Dyneema® HB 50 and Tensylon® HSBD 30A. They showed that a laminate with equal weight per cent of Tensylon® and Dyneema® had the lowest back face signature when compared to other configurations. Cline et al. [15] showed that a compliant matrix of Dyneema® HB212 allowed greater energy dissipation through fibre rotation resulting in higher ballistic limit velocity. Zhang et al. [16] fabricated multilayered UHMWPE composite laminates with no bonding between layers. It was realized that as the number of layers increased, the

https://doi.org/10.52202/081621-0002

energy absorption capacity of laminate increased. The projectile was also able to draw more material inside thereby delaying high tensile stresses on the back face of the laminate.

Few authors studied 7.62 mm projectiles with deformable cores. Carbajal et al. [17] determined the mechanical properties of a 7.62 × 39 mm mild steel core (MSC) projectile. They performed compression tests on all projectile components at various strain rates. The mechanical tests and an iterative numerical model generated a reliable set of mechanical properties data for numerical simulations. Crouch et al. [18] studied the impact of 7.62 × 39 mm MSC projectiles on boron carbide targets. They found that the jacket and filler increase the penetrating capacity of the projectile by damaging ceramic before the arrival of the core. The authors determined that the penetration event was a two-step process, i.e., mushrooming of the core near the ceramic surface and erosion of the core as it penetrates [18]. However, this understanding is more relevant to imbibe for hardened steel cores. Recently, Giglio et al. determined the mechanical properties of 7.62 × 51 mm lead core (LC) projectiles for numerical modelling, which provided acceptable results for the projectile's impact on an aluminium target [19,20].

There are many studies on the understanding of UHMWPE composite armour. However, a study on post-test analysis of UHMWPE composite after HVI with 7.62 mm deformable core projectiles was found missing in the open literature and thus it is performed in this study at IIT Delhi.

HVI tests were conducted on in-house fabricated armour panels using 7.62 × 51 mm LC and 7.62 × 39 mm MSC projectiles. Subsequently, an investigation was done to understand the damage to the panels using an ultrasonic scan. The armour was cut using a waterjet machine to visualize the projectile's travel in the armour. Also, recovered projectiles were studied on their nature of deformation. The insights from the experiments will be beneficial in the numerical and analytical modelling of the penetration process of these studied projectiles and UHWMPE composite armour.

2. MATERIALS AND METHODS

This section provides manufacturing details of armour plates along with details of test set-up.

2.1. UHMWPE Armour Plates

The UHMWPE armour plates were fabricated in-house from Honeywell Spectra Shield® (SS6472). A single ply of SS6472 is around 120 μm thick and contains four laminae. The fibres in SS6472 are arranged in $(0°/90°)_2$ configuration in a polyolefin-based matrix.

First, the required number of plies were cut and stacked. The stack was then placed in a compression moulding machine where mould temperature was maintained in a range of 128-132 °C. A pressure was then applied on the stack for 20 mins. Four similar panels were fabricated with an areal density (AD) of 14 kg m^{-2}. The panels had a planar area of more than 1000 cm^2. The panel had nominal dimensions of 300 mm × 350 mm.

2.2. Projectiles

The projectiles used are shown in Figure 1 and their details are listed in Table 1. Both 7.62 × 51 mm LC and 7.62 × 39 mm MSC projectiles contain deformable cores unlike hardened steel cores in armour-piercing (AP) projectiles [21,22]. Table 1 also shows the threat level of these projectiles according to IS 17051:2018 i.e. Indian personal body armour testing standard [23]. The initial kinetic energy of an LC projectile is 1.7 times of an MSC projectile. The core length of the MSC projectile is 20.8 mm.

https://doi.org/10.52202/081621-0002

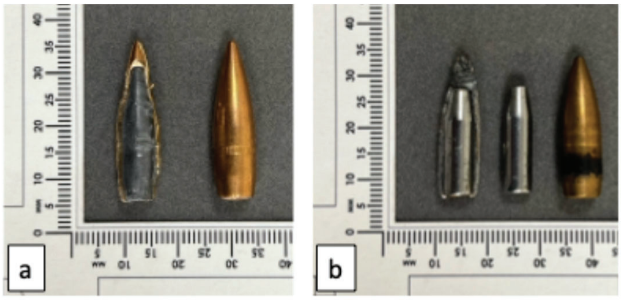

Figure 1. Projectiles used in this study (a) 7.62 × 51 mm LC and (b) 7.62 × 39 mm MSC

Table 1. Details of projectiles used in this study

Projectile	Weight (g)	Ordnance Velocity (m s^{-1})	Energy (J)	Core	IS 17051 *Threat Level*
7.62 × 39 mm MSC	7.45-8.05	710 ± 15	1953.39	Mild Steel	Level 2
7.62 × 51 mm LC	9.4-9.6	840 ± 15	3351.6	Lead	Level 3

2.3. High-velocity Impact Tests

The HVI tests were conducted at Terminal Ballistics Research Lab in Chandigarh, India as per IS 17051:2018 [23]. A schematic of the test set-up is shown in Figure 2. A weapon system was able to fire the required projectile is mounted ‘a’ distance from the target which in this case is 10 m. Also, between the weapon system and target, a velocity measurement system is present. The velocity measurement system is ‘b’ distance from the target which in this case is 2.5 m. The target is backed with Roma Plastilina No. 1 clay conditioned as per standard. Back-face signatures (BFS) are recorded on backing clay. There was at least a 51 mm distance on the panel between the shots as per IS 17051:2018.

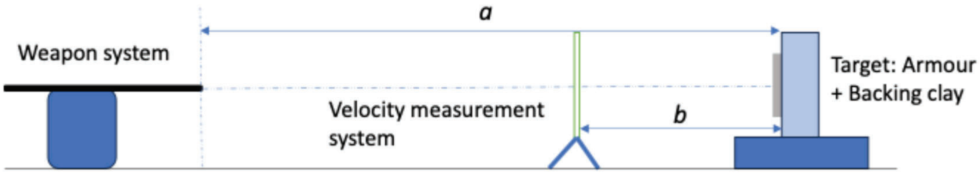

Figure 2. HVI test set-up

2.4. Post-Test Analysis

The BFS from each test was recorded on Roma Plastilina No. 1 clay after each test. The acceptable limit for BFS according to IS 17051:2018 is 25 mm for these projectiles. The ultrasonic sectional scan was performed using Olympus X3 equipment with a linear array transducer-receiver, glycerine was used as a medium for ultrasound wave propagation. Further, the armour panels were cut using a high-power waterjet machine. For UHMWPE panels subjected to the HVI test with 7.62 × 39 mm MSC projectile, reduced core length (RdCL) due to impact was also measured.

3. RESULTS AND DISCUSSIONS

3.1. BFS and Delamination

Results from HVI tests are presented in Table 2 and Table 3 for MSC and LC projectiles, respectively. It is quite apparent from these results that the BFS generated is considerably higher for LC projectiles than for MSC projectiles. Higher BFS will result in greater trauma to the user of armour. This signifies that with this armour design of UHMWPE composite, the user will endure greater trauma against LC projectiles. The high BFS values of LC projectiles can be attributed to the higher mass and velocity of these projectiles leading to almost double the kinetic energy of impact. It can be argued that BFS values of each shot is affected by prior shots on the clay. As this study followed IS 17051:2018 where although measurements of BFS are taken immediately after a shot but clay is not reset to default shape for the next shot.

Table 2. Results from HVI test for MSC projectile

MSC	HAP #1			HAP #2	
Shot No.	Velocity (m s^{-1})	BFS (mm)	RdCL (mm)	Velocity (m s^{-1})	BFS (mm)
1	711.3	11.9	13.6	714.7	10.2
2	715.8	7.4	14.2	715.3	8.5
3	714.9	4.0	15.1	712.5	6.5
4	715.7	4.6	16.4	713.5	5.2
5	714.5	4.6	15.3	715.9	5.0
6	708.2	1.5	14.1	714.9	5.2
7	722.8	3.3	14.6	715.8	4.0
8	715.1	2.7	14.9	715.1	6.1

Figure 3 also shows damage from both projectiles on similar panels. It is quite evident that, although both projectiles were defeated by UHMWPE composite panels, the delamination suffered in case of impact from the LC projectile was considerably more. Both panels delaminated into sub-laminates however, the number of sub-laminates was also higher in the case of LC projectiles.

Table 3. Results from HVI tests for LC projectile

LC	HAP #3			HAP #4	
Shot No.	Velocity (m s^{-1})	BFS (mm)	% Plies Perforated	Velocity (m s^{-1})	BFS (mm)
1	851.9	17.2	35.7	832.5	13.4
2	850.1	19.4	38.5	845.5	11.6
3	847.7	12.7	29.6	854.7	24.4
4	841.0	12.5	73.3	833.8	8.9
5	851.8	7.6	32.6	839.2	11.6
6	847.5	8.3	32.6	855.7	10.0
7	849.4	11.5	80.1	846.7	12.9
8	841.2	14.0	36.5	843.2	13.2

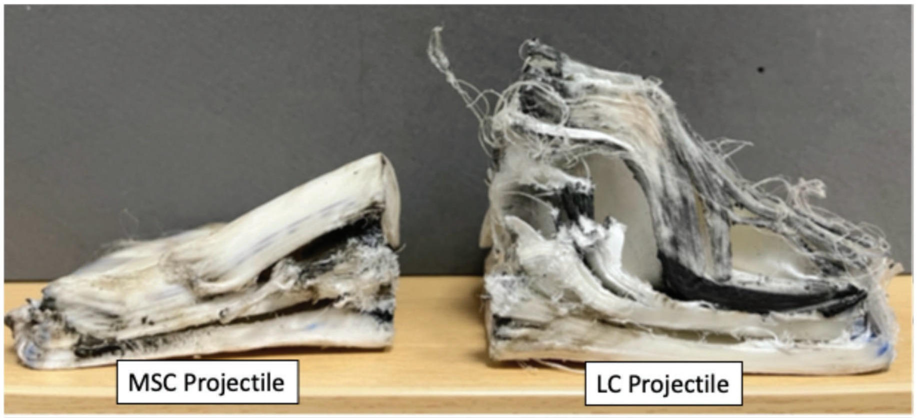

Figure 3. Delamination in UHMWPE composite panels due to impact from 7.62 mm projectiles with deformable cores

3.2. Post-Test Analysis

https://doi.org/10.52202/081621-0002

A typical LC projectile after the HVI test is shown in Figure 4. The LC projectile's lead deforms considerably around the copper jacket which also folds onto itself. On the other hand, the MSC projectile's mild steel deforms from the nose as shown in Figure 5. The nose is flattened and the final diameter at the nose side is much higher i.e. 8.6 ± 1.1 mm than the diameter at the shank (5.6 mm). The original diameter at the nose is 3.5 mm. Table 2 shows reduced core length RdCL for each shot for one panel only as the panel needs to be destroyed for it. The RdCL does not follow any trend with BFS and velocity. Also, the range of variation of RdCL values is limited between 13.6 and 16.4 mm. In contrast, core length reduction is quite a significant parameter in the defeat of hardened core projectiles [24]. Thus, the reduction in core length of the MSC projectile is insignificant in understanding the defeat of this projectile in UHMWPE composite panels at this velocity range.

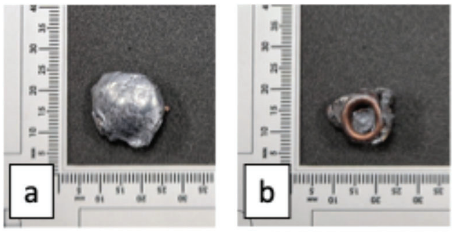

Figure 4. Typical state of 7.62 × 51 mm LC projectile

Figure 5. MSC cores from HAP #1 after the HVI test, cores are arranged in ascending shot order with the first one being the unused MSC core

Table 3 also shows the percentage of plies perforated with each shot in the case of LC projectile for one panel only as the panel needs to be destroyed for it. It was observed that LC projectiles were able to perforate the panel up to certain number of plies for each shot. The percentage of perforated plies was calculated by destructively opening the panel and taking a ratio of the weight of perforated plies to the weight of total panel. These values also do not seem to follow any trend with velocity and BFS and thus may be attributed to shot placement.

3.3. Ultrasonic Scan

A sectional ultrasonic scan was done to understand delamination from each shot. Figure 6 shows an ultrasonic scan of UHMWPE composite panels after HVI tests with 7.62 × 51 mm LC projectiles. In Figure 6 shot numbers are marked on the panel in black and the scanned region is marked in yellow along with arrows showing a relationship between them. Delamination after impact is quite evident in Figure 6. The colour from blue to red represents the intensity of the signal received. The faint blue contour at the bottom shows reflection from the back of the panel. The red contours show various places where delamination has occurred.

From Figure 3, it is apparent that the number of sub-laminates visible in the ultrasonic scan of Figure 6 is less. Since the signal gets dispersed due to such a high number of sub-laminates, only a few sub-laminates at the surface get registered in the ultrasonic scan. However, it is quite clear that near impact location a panel has undergone extensive delamination and will not provide effective ballistic resistance to the next shot.

Similarly, Figure 7 shows an ultrasonic scan of UHMWPE composite panels after HVI tests with 7.62 × 39 mm MSC projectiles. In the case of the MSC projectile, delamination in scans is like delamination visible in the sectional view shown in Figure 3. Also, it is apparent from Figure 7 that a lot more signals are captured shown in various shades of blue which can be attributed to the closeness of delaminated sub-laminates. It is quite clear from ultrasonic scans that although a panel may look intact after the HVI test, it will not have original stiffness after delamination, which weakens it against the next shot.

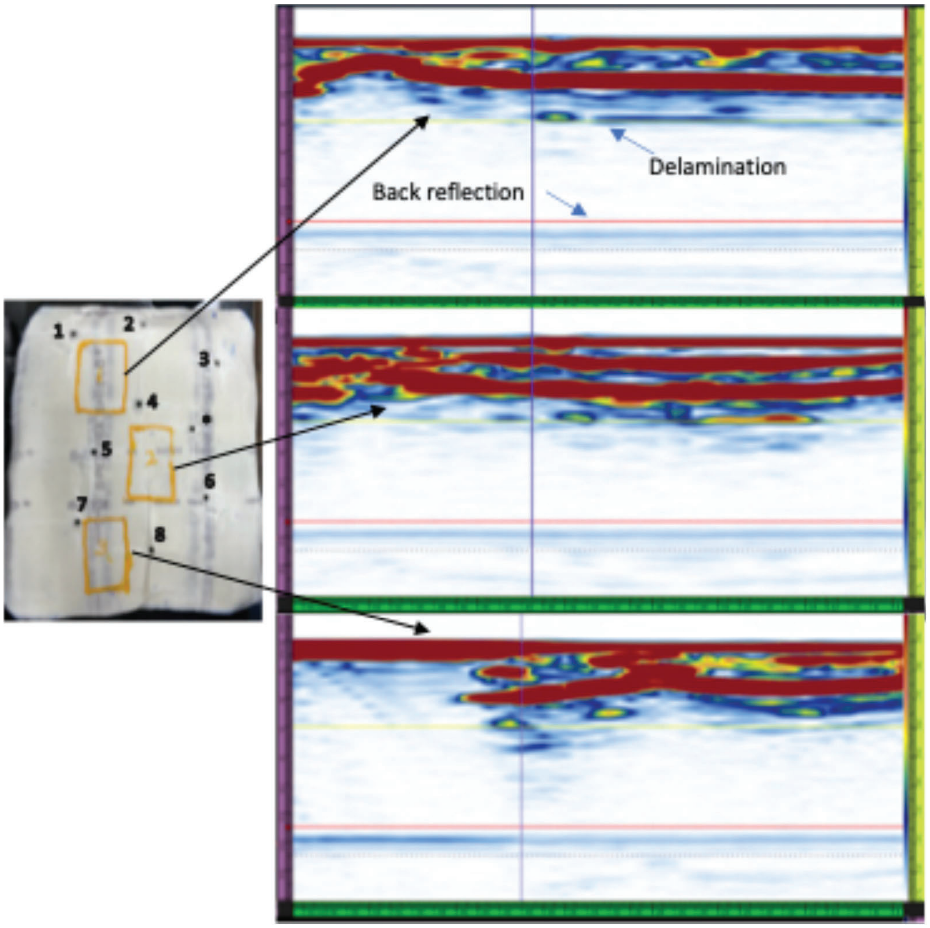

Figure 6. Ultrasonic scan of UHMWPE composite panels after HVI tests with 7.62 × 51 mm LC projectiles

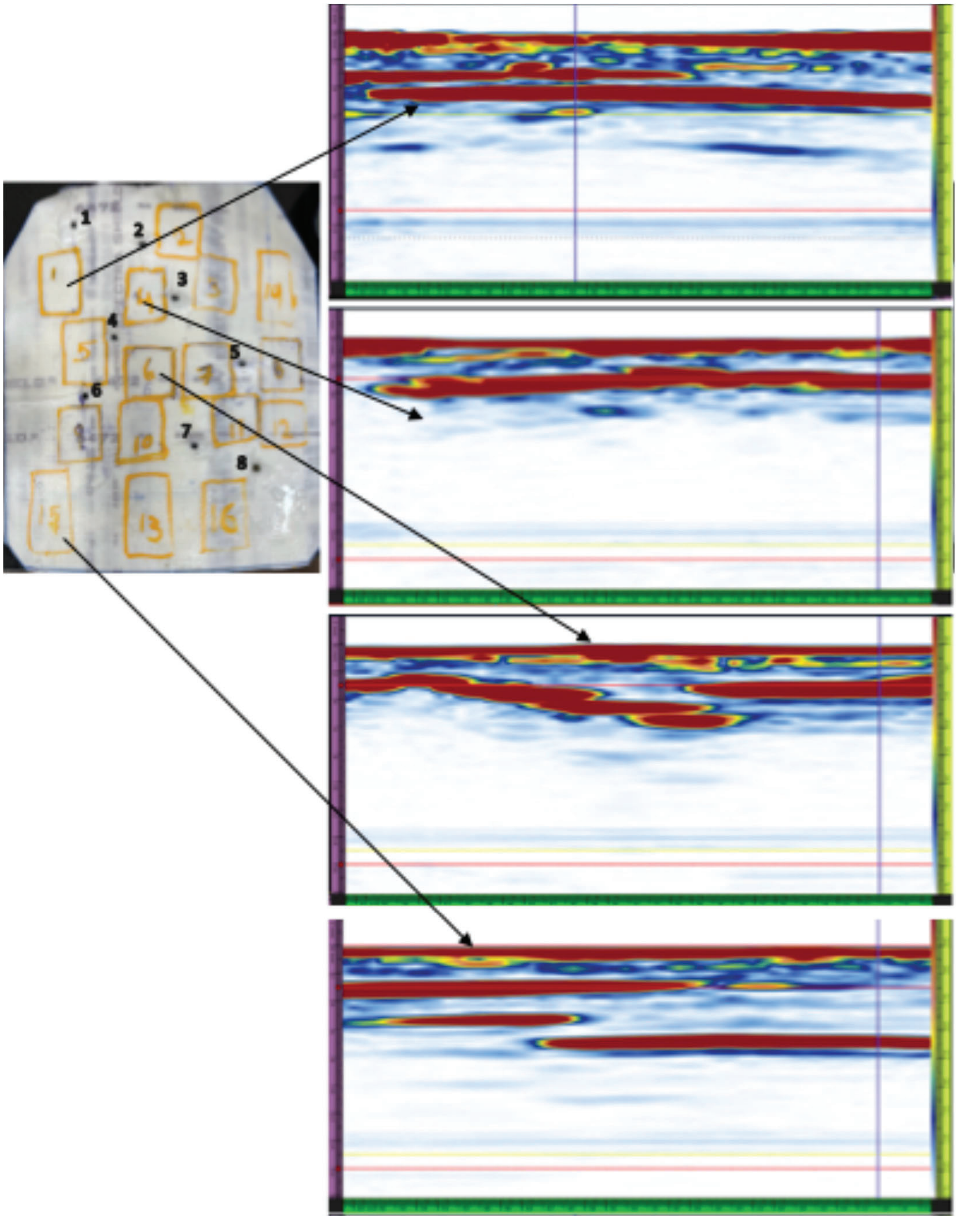

Figure 7. Ultrasonic scan of UHMWPE composite panels after HVI tests with 7.62 × 39 mm MSC projectiles

4. CONCLUSIONS

In this study, UHMWPE composite panels were subjected to HVI tests using 7.62 7.62 × 51 mm LC and 7.62 × 39 mm MSC projectiles. Subsequently, an investigation was done to understand the damage to the panels. The following conclusions can be drawn.

1. The BFS is higher for LC projectiles than for MSC projectiles which could be attributed to the higher initial energy of LC projectiles. Also, the number of delamination suffered by a UHMWPE composite panel is higher in the case of LC projectiles.
2. The reduced core length of the MSC projectile is not a significant parameter in determining the UHMWPE composite panel's ballistic resistance as is generally in the case of hardened core projectiles.

3. Similarly, number of plies perforated, in the case of LC projectiles, is dependent on shot placement.
4. Ultrasonic scan effectively shows delaminated areas in the case of both studied projectiles. However, an ultrasonic scan does not provide complete sectional detail which can only be studied after cutting the panel.
5. Future work can use inferences from this work like the number of sub-laminates in a section, delaminated areas or core deformation, for robust numerical analysis.

Acknowledgements

The authors acknowledge the use of manufacturing facilities at the Centre of Excellence in Personal Body Armour at the Indian Institute of Technology Delhi and testing facilities at Terminal Ballistics Research Lab DRDO Chandigarh.

References

[1] Bhatnagar A. Lightweight Ballistic Composites: Military and Law-Enforcement Applications: Second Edition. 2016. https://doi.org/10.1016/C2014-0-03657-X.

[2] Crouch IG. Body armour – New materials, new systems. Defence Technology 2019;15:241–53. https://doi.org/10.1016/j.dt.2019.02.002.

[3] O'Masta MR, Crayton DH, Deshpande VS, Wadley HNG. Mechanisms of penetration in polyethylene reinforced cross-ply laminates. Int J Impact Eng 2015;86:249–64. https://doi.org/10.1016/j.ijimpeng.2015.08.012.

[4] Nguyen LH, Ryan S, Cimpoeru SJ, Mouritz AP, Orifici AC. The effect of target thickness on the ballistic performance of ultra-high molecular weight polyethylene composite. Int J Impact Eng 2015;75:174–83. https://doi.org/10.1016/j.ijimpeng.2014.07.008.

[5] Greenhalgh ES, Bloodworth VM, Iannucci L, Pope D. Fractographic observations on Dyneema® composites under ballistic impact. Compos Part A Appl Sci Manuf 2013;44:51–62. https://doi.org/10.1016/j.compositesa.2012.08.012.

[6] O'Masta MR, Deshpande VS, Wadley HNG. Defect controlled transverse compressive strength of polyethylene fibre laminates. Int J Solids Struct 2015;52:130–49. https://doi.org/10.1016/j.ijsolstr.2014.09.023.

[7] Lässig TR, May M, Heisserer U, Riedel W, Bagusat F, van der Werff H, et al. Effect of consolidation pressure on the impact behaviour of UHMWPE composites. Compos B Eng 2018;147:47–55. https://doi.org/10.1016/j.compositesb.2018.04.030.

[8] Lee BL, Song JW, Ward JE. Failure of Spectra®* Polyethylene Fiber-Reinforced Composites under Ballistic Impact Loading. J Compos Mater 1994;28:1202–26. https://doi.org/10.1177/002199839402801302.

[9] Taylor SA, Carr DJ. Post-failure analysis of 0°/90°ultra high molecular weight polyethylene composite after ballistic testing. J Microsc 1999;196:249–56. https://doi.org/10.1046/j.1365-2818.1999.00632.x.

[10] Karthikeyan K, Russell BP, Fleck NA, Wadley HNG, Deshpande VS. The effect of shear strength on the ballistic response of laminated composite plates. European Journal of Mechanics - A/Solids 2013;42:35–53. https://doi.org/10.1016/j.euromechsol.2013.04.002.

[11] Heisserer U, Van Der Werff H, Hendrix J. Ballistic depth of penetration studies in Dyneema® composites. Proceedings - 27th International Symposium on Ballistics, BALLISTICS 2013 2013;2:1936–43.

[12] Nguyen LH, Ryan S, Cimpoeru SJ, Mouritz AP, Orifici AC. The effect of target thickness on the ballistic performance of ultra-high molecular weight polyethylene composite. Int J Impact Eng 2015;75:174–83. https://doi.org/10.1016/j.ijimpeng.2014.07.008.

[13] Lässig TR, May M, Heisserer U, Riedel W, Bagusat F, van der Werff H, et al. Effect of consolidation pressure on the impact behaviour of UHMWPE composites. Compos B Eng 2018;147:47–55. https://doi.org/10.1016/j.compositesb.2018.04.030.

[14] Reddy PRS, Reddy TS, Srikanth I, Kushwaha J, Madhu V. Development of cost effective personnel armour through structural hybridization. Defence Technology 2020;16:1089–97. https://doi.org/10.1016/j.dt.2019.12.004.

[15] Cline J, Love B. The effect of in-plane shear properties on the ballistic performance of polyethylene composites. Int J Impact Eng 2020;143. https://doi.org/10.1016/j.ijimpeng.2020.103592.

[16] Zhang R, Han B, Zhong JY, Qiang LS, Ni CY, Zhang Q, et al. Enhanced ballistic resistance of multilayered cross-ply UHMWPE laminated plates. Int J Impact Eng 2022;159:104035. https://doi.org/10.1016/j.ijimpeng.2021.104035.

[17] Carbajal L, Jovicic J, Kuhlmann H. Assault riffle bullet-experimental characterization and computer (FE) modelling. Conference Proceedings of the Society for Experimental Mechanics Series 2011;6:647–64. https://doi.org/10.1007/978-1-4614-0222-0_77.

[18] Crouch IG, Appleby-Thomas G, Hazell PJ. A study of the penetration behaviour of mild-steel-cored ammunition against boron carbide ceramic armours. Int J Impact Eng 2015;80:203–11. https://doi.org/10.1016/j.ijimpeng.2015.03.002.

[19] Peroni L, Scapin M, Fichera C, Manes A, Giglio M. Mechanical properties at high strain-rate of lead core and brass jacket of a NATO 7.62 mm ball bullet. EPJ Web Conf, vol. 26, 2012. https://doi.org/10.1051/epjconf/20122601060.

[20] Giglio M, Gilioli A, Manes A, Peroni L, Scapin M. Investigation about the influence of the mechanical properties of lead core and brass jacket of a NATO 7.62 mm ball bullet in numerical simulations of ballistic impacts. EPJ Web Conf, vol. 26, 2012. https://doi.org/10.1051/epjconf/20122604010.

[21] Carbajal L, Jovicic J, Kuhlmann H. Assault riffle bullet-experimental characterization and computer (FE) modelling. Conference Proceedings of the Society for Experimental Mechanics Series 2011;6:647–64. https://doi.org/10.1007/978-1-4614-0222-0_77.

[22] Kiliç N, Ekici B. Ballistic resistance of high hardness armour steels against 7.62 mm armour piercing ammunition. Mater Des 2013;44:35–48. https://doi.org/10.1016/j.matdes.2012.07.045.

[23] Bureau of Indian Standards. Textiles — Bullet Resistant Jackets — Performance Requirements. IS 17051 : 2018 2018.

[24] Kartikeya K, Chouhan H, Ram K, Prasad S, Bhatnagar N. Ballistic evaluation of steel/UHMWPE composite armour system against hardened steel core projectiles. Int J Impact Eng 2022;164:104211. https://doi.org/10.1016/j.ijimpeng.2022.104211.